# CrystEngComm

Accepted Manuscript






ROYAL SOCIETY OF CHEMISTRY

www.rsc.org/crystengcomm

Cite this: DOI: 10.1039/c0xx00000x

www.rsc.org/xxxxxx

ARTICLE TYPE

# Organic-inorganic hybrid assemblies based on Ti-substituted polyoxometalates for photocatalytic dye degradation

Li-Jie Xu, Wen-Zhe Zhou, Li-Yuan Zhang, Bin Li, Hong-Ying Zang*, Yong-Hui Wang, Yang-Guang Li*

***Received (in XXX, XXX) Xth XXXXXXXXX 20XX, Accepted Xth XXXXXXXXX 20XX***

**DOI: 10.1039/b000000x**

Two new organic-inorganic hybrid compounds, $[N(CH_3)_4]_6[Cu^{II}Lo][(Ti_2O)(PW_{11}O_{39})_2]\cdot 4H_2O$ (**1**) and $[N(CH_3)_4]_2[H_2bpp]_2[Cu^{II}Lo][(Ti_2O)(PW_{11}O_{39})_2]\cdot 1.5H_2O$ (**2**) (*Lo* = 1,2-bis(3-(2-pyridyl)pyrazole-1-ylmethyl)benzene, bpp = 1,3-bis(4-piperidyl)propane), based on Ti-substituted polyoxometalates (*abbr.* Ti-POMs) and the metal-organic linking units constructed by $Cu^{II}$ ions and bichelate-bridging ligands (*Lo*), have been hydrothermally prepared. The two compounds were characterized by elemental analyses, IR spectra, TG analyses, XPS spectra, power X-ray diffraction and single-crystal X-ray diffraction analyses. Both compounds contain a rare corner-sharing double-Keggin type POM architecture in the Ti-POM species. In **1** and **2**, the double-Keggin-type polyoxoanions connect with the butterfly-type $[Cu^{II}Lo]$ units to form a 1-D chain and a square plane, respectively. The photocatalytic properties of compounds **1-2** were investigated with the methylene blue (MB) degradation model under UV irradiation, indicating good photocatalytic activities. Furthermore, to compare the photocatalytic property of the Keggin-type Ti-POMs with those of traditional Keggin-type POMs, another compound $[Cu^{I}Lo]_4[PW_{12}O_{40}]$ **(3)** was synthesized by combining typical Keggin-type polyoxoanions with the metal-organic $[Cu^{I}Lo]$ units. A series of MB degradation experiments suggest that the Ti-POMs exhibit better photocatalytic activity than those of typical Keggin-type saturated POM species.

## Introduction

The design and synthesis of organic-inorganic hybrid materials based on polyoxometalates (POMs) and metal-organic units have been paid great attention in last two decades. The introduction of various POM units into the metal-organic coordination polymer systems have not only dramatically expanded the structural topologies of hybrid materials, but also endowed them new functionalities and potential applications in catalysis, adsorption, luminescent, electronic and magnetic materials.[1-5] Recently, a concentrating research topic in this field is the exploration of new photocatalytic systems for the dye degradation.[6-15] Generally, the POM-based metal-organic hybrid materials possess at least three advantages as the photocatalytic candidates: Firstly, POMs usually display photo-sensitive activity, which is similar to those of photo-sensitive semi-conductor materials for example titanium dioxide ($TiO_2$). Under UV irradiation, these materials can generate electrons to activate the hydroxyl radicals in water and then degrade the organic dye molecules.[16] Secondly, the combination of POM units and metal-organic complex fragments can dramatically decrease the solubility of these composite materials, which can transfer soluble POM units into heterogeneous catalytic system, promoting the recycling of POM catalysts and eliminating the secondary water pollution. Thirdly, POMs and metal-organic moieties provide a dynamic molecular library to construct numerous hybrid assemblies, representing an ideal system to design and select active photocatalysts for the dye degradation. So far Keggin/Dawson-type POM-based hybrid complexes are one of the most developed catalyst systems for dye degradation.[6-15] However, it is still difficult to evaluate that which type of POMs possess better photocatalytic activities due to different catalytic conditions and various composition and combination modes between POMs and numerous metal-organic species. Thus, an ongoing challenging project in this research filed is chemically modulating the addenda atoms of POMs with different metal ions and setting them in a similar hybrid system so as to evaluate the photocatalytic activity of different POM species and select more active photocatalysts. Ti-substituted POMs (*abbr.* Ti-POMs) has ever been estimated as a potentially effective photocatalyst species based on the DFT calculation.[17] Furthermore, $H_3PW_{12}O_{40}/TiO_2$ composite materials have exhibited high photocatalytic activities in the degradation process.[16] Therefore, the exploration of Ti-POM-based organic-inorganic hybrid compounds may suggest a new way to obtain active photocatalyst systems.

Based on above consideration, we attempt to design and synthesis of Ti-POM-based organic-inorganic hybrid assemblies. To date, Ti-POM architectures have been constructed by a series of lacunary POM units, such as $\{PW_{11}\}$, $\{PW_{10}\}$, $\{PW_9\}$, $\{P_2W_{17}\}$ and $\{P_2W_{15}\}$.[18-25] Many Ti-POMs are water soluble but unstable in aqueous solution, which are difficult to use as synthetic precursors to construct hybrid compounds. So far Ti-POM-based organic-inorganic hybrid compounds have not been reported yet. In this work, a {Cu*Lo*} (*Lo* = 1,2-bis(3-(2-pyridyl)pyrazole-1 -ylmethyl)benzene) metal-organic complex is used to combine with Ti-POM species. We have ever proved that such a butterfly-type {Cu*Lo*} motif exhibits quite flexible and active coordination capability to the surface oxygen atoms of POM species,[26] which may stabilize the metastable POM species during the hydrothermal reaction process and tend to obtain crystalline hybrid compounds. Herein, we reported two new hybrid

compounds, $[N(CH_3)_4]_6[Cu^{II}Lo][(Ti_2O)(PW_{11}O_{39})_2]\cdot 4H_2O$ (**1**) and $[N(CH_3)_4]_2[H_2bpp]_2[Cu^{II}Lo][Ti_2O(PW_{11}O_{39})_2]\cdot 1.5H_2O$ (**2**) (bpp = 1,3-bis(4-piperidyl) propane). Both compounds contain a corner-sharing double-Keggin-type POM architecture, which is observed for the first time in the Ti-substituted POM species. In **1** and **2**, the double-Keggin-type polyoxoanions connect with the butterfly-type $[Cu^{II}Lo]$ units to form an infinite chain and a square plane, respectively. To our knowledge, compounds **1** and **2** represent the first examples of hybrid compounds based on Ti-POMs under hydrothermal synthetic conditions. The photocatalytic properties of compound **1**-**2** were investigated with the catalytic model of methylene blue (MB) degradation under UV light. Furthermore, another hybrid compound $[Cu^{I}Lo]_4[PW_{12}O_{40}]$ **(3)** was also synthesized as a reference sample to compare with the photocatalytic property of Ti-POM species.

**Table 1.** Crystal data and structure refinement for **1**-**2**.

| Compounds | 1 | 2 |
|---|---|---|
| Formula | $C_{48}H_{100}N_{12}O_{83}P_2Ti_2W_{22}Cu$ | $C_{58}H_{79}N_{12}O_{80.50}P_2Ti_2W_{22}Cu$ |
| *M*r | 6439.38 | 6498.31 |
| *T*/K | 296(2) | 296(2) |
| Cryst. Syst. | Monoclinic | Triclinic |
| Space group | $P2_1/n$ | $P$-1 |
| *a*/Å | 12.9068(5) | 14.6474(9) |
| *b*/Å | 23.7447(9) | 19.8814(12) |
| *c*/Å | 38.8170(17) | 21.9641(14) |
| $\alpha$ (°) | 90 | 78.8740(10) |
| $\beta$ (°) | 96.4510(10) | 88.1130(10) |
| $\gamma$ (°) | 90 | 75.6590(10) |
| *V*/Å$^3$ | 11820.8 (8) | 6079.7(7) |
| Z | 4 | 2 |
| $\mu$/mm$^{-1}$ | 21.74 | 21.136 |
| *F*(000) | 11468 | 5772 |
| Refls | 67885 | 35214 |
| $R_{int}$ | 0.0815 | 0.0606 |
| GOF | 1.006 | 1.061 |
| $R_1$ [$I > 2\sigma(I)$]$^a$ | 0.0526 | 0.0645 |
| w $R_2$(all data)$^b$ | 0.1213 | 0.1882 |
| $\Delta\rho_{max,min}$/e Å$^{-3}$ | 3.065 and -3.332 | 3.12 and -2.593 |

Note: $^aR_1 = \Sigma||F_o| - |F_c||/\Sigma|F_o|$; $^bwR_2 = \Sigma[w(F_o^2 - F_c^2)^2]/\Sigma[w(F_o^2)^2]^{1/2}$.

## Experimental

### Materials and physical measurement

All reagents and solvents for the synthesis were purchased commercially and used without further purification. The POM $[(CH_3)_4N]_7[PTi_2W_{10}O_{40}]\cdot 4H_2O$ was synthesized according to the literature.[27] The bichelate-bridging ligand L*o* was prepared by the reaction of 1,2-bis(bromomethyl)benzene with 3-(2-pyridyl)pyrazole according to the reported method.[28] Elemental analyses (C, H and N) were performed by using a Perkin-Elmer 2400 CHN elemental analyzer. Cu, Ti and W contents were determined by using a Leaman inductively coupled plasma (ICP) spectrometer. The FT-IR spectra were analyzed from KBr pellets in the range 4000-400 cm$^{-1}$ using a Mattson Alpha-Centauri spectrometer. Thermogravimetric analyses (TGA) were performed on a Perkin-Elmer TG-7 analyzer heated from 50-800 $^o$C at a heating rate of 10 $^o$C/min under nitrogen atomosphere. Powder X-ray diffraction (PXRD) measurements were performed by using a Rigaku D/max-□B X-ray diffractometer at a scanning rate of 1° min$^{-1}$ ranging from 5-45° and with Cu K$\alpha$ radiation ($\lambda$ = 1.5418 Å). Photocatalytic experiment was conducted in a 500 mL water-cooled cylindrical quartz container. The catalyst sample (40 mg) was added into the 400 mL 10.0 mg L$^{-1}$ methylene blue (MB) solution, magnetically stirred in the dark for ca. 10 min. Then, the above mixture was transferred to the quartz container irradiated under a high-pressure 125 W mercury lamp. The mixture was kept stirring during irradiation. 3 mL liquid sample was taken out and analyzed by using a UV-7502PC UV/Vis spectrophotometer in every 5 min.

### Synthesis

**$[N(CH_3)_4]_6[Cu^{II}Lo][(Ti_2O)(PW_{11}O_{39})_2]\cdot 4H_2O$** (**1**). $[(CH_3)_4N]_7[PTi_2W_{10}O_{40}]\cdot 4H_2O$ (0.3125g, 0.1 mmol) and CuCl (0.05g, 0.5mmol) were mixed in 10 mL distilled water with continuous stirring at room temperature for 30 min. The pH value of the above mixture was adjusted to ca. 3.0 with 1M HCl. Then, the above mixture and L*o* (0.039g, 0.1mmol) ligand were put into a Teflon-lined autoclave. The reaction system was kept under autogenous pressure at 180 $^o$C for 5 days. After slowly cooling to

room temperature, green block crystals were filtered and washed with distilled water (50% yield based on W). Anal. Calcd for $C_{49}H_{100}N_{11}O_{83}P_2Ti_2W_{22}Cu$: C 9.08, H 1.61, N 2.58, Cu 1.01, Ti 1.40, W 62.91. Found: C 8.95, H 1.55, N 2.61, Cu 0.94, Ti 1.49, W 62.84. Selected IR (KBr pellet, $cm^{-1}$): 3417(s), 3136(w), 1614(s), 1504(s), 1444(m), 1386(s), 1334(s), 1232(s), 1162(s), 1069(m), 966(w), 892(m), 810(w).

**$[N(CH_3)_4]_2[H_2bpp]_2[Cu^{II}Lo][Ti_2O(PW_{11}O_{39})_2]\cdot 1.5H_2O$ (2)**. $[(CH_3)_4N]_7[PTi_2W_{10}O_{40}]\cdot 4H_2O$ (0.1563 g, 0.05 mmol) and CuCl (0.05g, 0.5mmol) were mixed in 10 mL distilled water and stirred at room temperature for 30 min. The pH of the above mixture was adjusted to ca. 3.0 with 1M HCl. Then, the above mixture, L*o* (0.02g, 0.05mmol) and bpp (0.01g, 0.05mmol) were transferred into a Teflon-lined autoclave, kept under autogenous pressure at 180 °C for 5 days. After slowly cooling to room temperature, deep green block crystals were filtered and washed with distilled water (40% yield based on W). Anal. Calcd for $C_{58}H_{79}N_{12}O_{80.50}P_2Ti_2W_{22}Cu$: C 10.71, H 1.32, N 2.44, Cu 0.86, Ti 1.40, W 62.37. Found: C 10.72, H 1.22, N 2.59, Cu 0.93, Ti 1.47, W 62.24. Selected IR (KBr pellet, $cm^{-1}$): 3447(s), 3141(s), 1614(s), 1504(s), 1444(m), 1389(s), 1336(s), 1234(s), 1071(w), 969(w), 891(w), 809(w).

### X-ray crystallography

The crystallographic data were collected at 296K on the Bruker Apex CCD diffractometer using graphite monochromatic Mo Kα radiation (λ = 0.71073 Å). A multi-scan absorption correction was applied. The crystal data were solved by the direct method and refined by a full-matrix least-squares on $F^2$ using the SHELXTL-97 program.[29] During the refinement of compounds **1-2**, all non-hydrogen atoms were refined anisotropically. The H atoms on organic carbon centers were fixed in calculated positions. Furthermore, the restraint commands "ISOR" and "SIMU" were used to restrain some non-H atoms with ADP or NPD problems in the crystal structures of **1-2**. Moreover, some six-member and five-member rings of the L*o* ligands in **1-2** were also restrained with the "DFIX", "AFIX" and "DELU" commands. All above restrained refinement led to relatively high restraint values 138 and 848 for compound **1** and **2**, respectively. In the final refinement, the contributions of disordered solvent to the structure factors in compound **1** were removed with the SQUEEZE program[30] and the crystal structure was then further refined with new hkl file generated by the SQUEEZE calculation. Based on the elemental analysis, TG analysis and the SQUEEZE calculation results, another three water molecules were directly included in the final molecular formula of **1**. Crystal data and structure refinement for **1-2** are list in Table 1. Selected bond lengths and angles for **1-2** are listed in the Supporting Information, Tables S1-S2.

## Results and discussion

### Synthesis

During the synthesis, several important synthetic factors should be emphasized: i) The pH of the initial reaction mixture should be carefully controlled in the range of 3.0 – 3.5, otherwise, no Ti-substituted POMs can be isolated from the synthetic system. When the pH is adjusted from 3.5 to 5.0, the Keggin-type POM unit $[PW_{12}O_{40}]^{3-}$ is isolated from the reaction system (see the synthesis of compound **3** in ESI). It is speculated that the double-Keggin-type POM unit $[Ti_2O(PW_{11}O_{39})_2]^{8-}$ might be just stable in the pH range of 3.0 – 3.5. ii) The CuCl should be used as the copper ion sources while not $CuCl_2$. During the reaction process, CuCl is less soluble in water at room temperature. However, in the hydrothermal reaction system, the Cu(I) can be slowly oxidized into soluble Cu(II) ions by the mixed $O_2$ from air. These *in situ* generated Cu(II) ions are coordinated with the bichelate-bridging ligand L*o*, forming the $[CuLo]^{2+}$ fragment and then assembling with the double-Keggin-type POM clusters. However, when the Cu(II) ions were directly added in the reaction system, only blue amorphous powders were obtained. It is presumed that the reactions between soluble Cu(II) ions and Ti-substituted POMs may be too quick and large initial Cu(II) ions just led to precipitates while not crystalline products. iii) The organic L*o* ligands should be directly placed under the bottom of the autoclave and then the initial mixture containing POM and CuCl was directly covered on the L*o* ligands. Since the organic ligand is insoluble in water, it is unnecessary to pre-mix L*o* with POM and CuCl in aqueous solution. Otherwise, such organic ligand will stick on the glass wall and decrease the final yield of the crystalline products **1-2**. iv) The reaction temperature should be above 180 °C in order to prompt the solubility of the organic ligands. Below 180 °C, no crystalline sample can be obtained. v) The introduction of bpp ligand into the reaction system initially intended to change the metal-organic fragments, however, such ligands just led to the different assembling modes between POM units and the [CuL*o*] fragments in compounds **1** and **2**. Based on the structural features of **1** and **2**, it is presumed that the protonated bpp ligands might affect the orientations of [CuL*o*] units in the double-Keggin-type POM clusters, leading to the different final assemblies.

### Crystal structures of 1–2

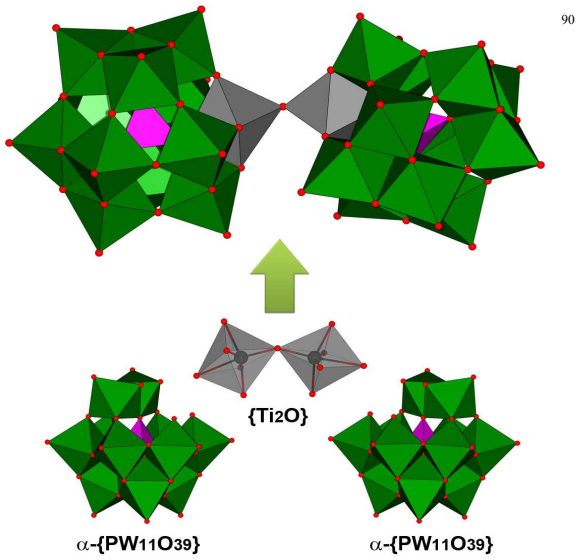


**Fig. 1** Polyhedral view of the double-Keggin-type polyoxoanion in **1** and **2**.

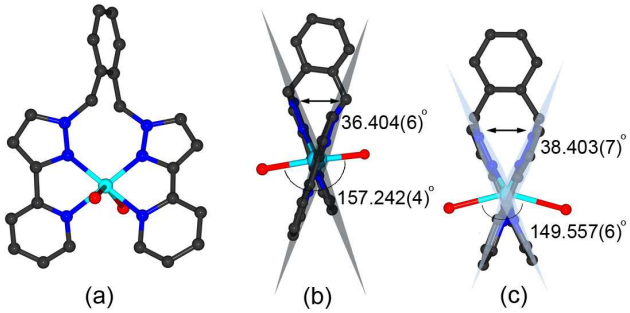

**Fig. 2 (a)** Ball-and-stick view of [$Cu^{II}$L*o*] unit in **1** and **2**; Side view of [$Cu^{II}$L*o*] unit in **1 (b)** and **2 (c)**, showing the different dihedral angles and O-Cu-O angles.

The single crystal X-ray diffraction analysis showed that both compounds contain a double-Keggin-type POM unit (Fig. 1) and a butterfly-type [CuL*o*] metal-organic moiety (Fig. 2). The POM architecture can be viewed as two α-Keggin-type units linking together via a corner-sharing mode. According to the composition of such POM moiety, this POM unit can be separated into three parts, that is, two monovacant Keggin-type α-{$PW_{11}O_{39}$} fragments and one {$Ti_2O$} bridge (Fig. 1). The vacant site of each α-{$PW_{11}O_{39}$} unit is occupied by the Ti center and two vacant POM units link together via the {Ti-O-Ti} bridge. The bond lengths of Ti-O range from 1.758(13) to 2.427(17) Å for **1** and range from 1.797(18) to 2.365(16) Å for **2**, respectively. The bond angles of Ti-O-Ti are 158.7(8)° for **1** and 149.0(12) ° for **2**, respectively. These bond lengths and angles are quite similar to the reported Ti-substituted polyoxotungstates.[18-25] It is worth mentioning that {Ti-O-Ti} bridge is a common fragment in most of the reported Ti-substituted polyoxotungstates. However, the vacant POM units are always linked together by multiple {Ti-O-Ti} bridges.[18-25] In this case, the double-Keggin skeleton is only connected by one {Ti-O-Ti} linker, which is observed for the first time in the Ti-substituted POM species.

The butterfly-type [CuL*o*] coordination unit can be viewed as a Cu(II) center surrounding with a four-dentate chelate ligand. The oxidation state of the Cu(II) center was confirmed by the bond-valence sum (BVS) calculation, six-coordinated environment, and the green coloration of the crystals. In both compounds, the Cu(II) center is six-coordinated with four N atoms derived from one L*o* ligand and two terminal oxygen atoms from two adjacent double-Keggin-type polyoxoanions (Fig. 2). The bond lengths of Cu-N are in the range of 1.953(16)-2.052(17) Å for **1** and 1.937(16)-2.029(17) Å for **2**, and those of Cu-O are 2.475(5)-2.766(7) Å for **1** and 2.639(6)-2.684(3) Å for **2**, respectively. It is found that the pypz groups in the [CuL*o*] unit are not in the same plane, and the dihedral angels between two pypz groups are 36.404(6)° for **1** and 38.403(7)° for **2**, respectively (Fig. 2). Furthermore, the O-Cu-O angles of the [CuL*o*] units are 157.242(4) ° for **1** and 149.557(2) ° for **2**, respectively. Such differences may lead to various assembling modes between [CuL*o*] and double-Keggin-type POM units in **1** and **2**.

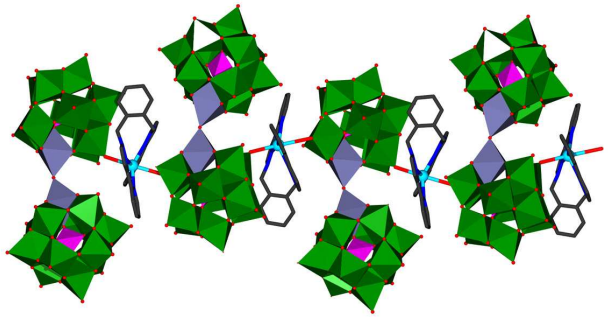

**Fig. 3** 1-D chain in **1** based on [$Cu^{II}$L*o*] and [$(Ti_2O)(PW_{11}O_{39})_2$]$^{8-}$ units.

Compound **1** crystallizes in the monoclinic space group $P2_1/n$. The basic structural unit contains a double-Keggin-type polyoxoanion [$(Ti_2O)(PW_{11}O_{39})_2$]$^{8-}$ , a [CuL*o*]$^{2+}$ moiety and six [$N(CH_3)_4$]$^+$ cations (Fig. S1, ESI). In **1**, the [CuL*o*] and POM units alternately link together to form a 1-D chain (Fig. 3 and Fig. S2, ESI). In such a chain, only one Keggin-type part of POM clusters is used to link with [CuL*o*] fragments, assembling into a helical chain. In the packing arrangement, all the 1-D chains are parallel with each other along *b* axis (Fig. S3, ESI). There are no obvious intermolecular interactions between two adjacent chains. The counter cations [$(CH_3)_4N$]$^+$ and lattice water molecules reside in the interspaces formed by these hybrid chain units.

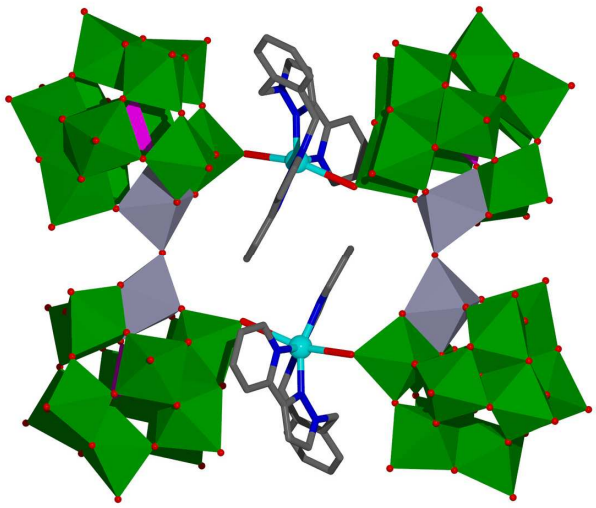

**Fig. 4** Square plane cluster in **2** based on [$Cu^{II}$L*o*] and [$(Ti_2O)(PW_{11}O_{39})_2$]$^{8-}$ units.

Compound **2** crystallizes in the triclinic space group *P*-1. The basic structural unit contains one double-Keggin-type polyoxoanion [$(Ti_2O)(PW_{11}O_{39})_2$]$^{8-}$, one [CuL*o*]$^{2+}$ fragment, two [$N(CH_3)_4$]$^+$ and two protonated bpp ligands (Fig. S4, ESI). In **2**, two double-Keggin-type polyoxoanions [$(Ti_2O)(PW_{11}O_{39})_2$]$^{8-}$ and two [$Cu^{\square}$L*o*] units link together, forming a molecular square plane (Fig. 4, Fig. S5, ESI). The molecular square plane is central symmetric and the symmetric center resides in the center of the square plane. In comparison with the structure of **1**, both Keggin parts of the POM clusters attend the assembly of final molecular square plane. In the packing arrangement, all these molecular square planes adopt the same orientation and are parallel with each other on the *bc* plane (Fig. S6, ESI). There are no obvious intermolecular interactions between two adjacent hybrid clusters. The [$(CH_3)_4N$]$^+$ cations, protonated bpp ligands and lattice water molecules reside in the interspaces formed by the molecular square moieties of **2**.

### Photocatalytic properties

Nowadays effectively decomposing waste organic molecules plays a crucial role in environment pollution.[31] Methylene blue (MB) is often employed as a typical model dye contaminant to estimate the photocatalytic effectiveness of POMs.[6,9] It is known that a wide range of POMs possess photocatalytic activities in the degradation of organic dyes under UV irradiation. Herein, we want to investigate the photocatalytic activitity of Ti-substituted Keggin-type polyoxotungstates. However, Ti-substituted POM salts are generally water-soluble and less stable in water, which may induce the secondary pollution if they are directly used as photocatalysts for the above purpose. So we prepared POM-based inorganic-organic hybrid compounds to decrease the solubility of catalysts. Furthermore, compound **3,** [Cu(I)L*o*]$_4$[$PW^{V}W^{VI}_{11}O_{40}$], consisting of the typical Keggin units and the metal-organic complex was synthesized and used for comparison. The synthesis and structures for compound **3** was shown in the supporting information. Moreover, the blank MB aqueous solution without any catalyst was also checked as the control experiments. In the process, MB (400 mL, 10.0 mg $L^{-1}$) combined with the catalyst (compounds **1**-**3**; 40 mg) were exposed to UV light (125 W). 3

mL of the upper clear liquid was taken out from the beaker every 5 min for UV-vis analysis.

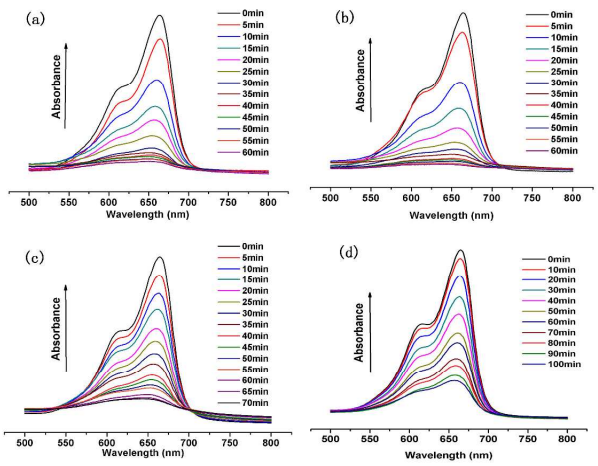


**Fig. 5** Absorption spectra of the MB aqueous solution during the photodegradation under UV light irradiation with (a) **1**, (b) **2**, (c) **3**, (d) no catalyst.

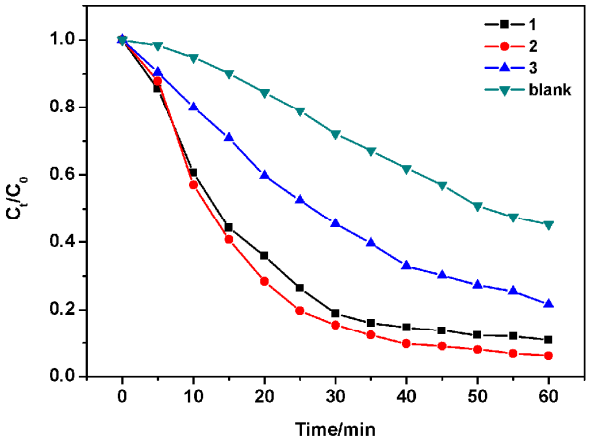


**Fig. 6** Plot of $C_t/C_0$ of MB versus reaction time.

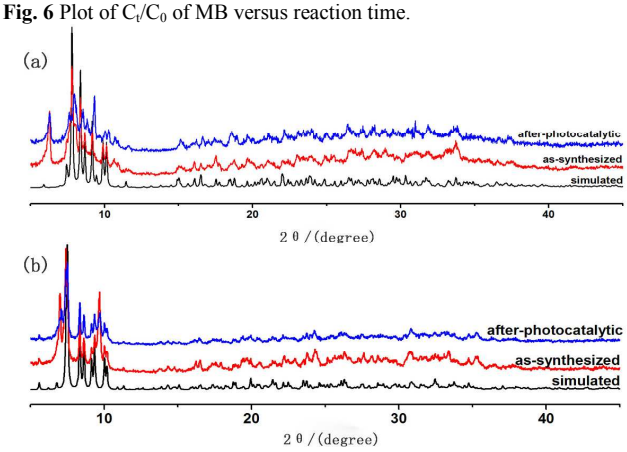


**Fig. 7** The PXRD patterns of compound **1(a)** and **2(b)** with simulated (black, below), as-synthesized (Orange) and blue lines (after four-circle of catalytic process)

As shown in Fig. 5, those in the presence of **1-2** dramatically decreased nearly the same level only within 60 min under UV irradiation. However, it takes 70 minutes for compound **3** to degrade. Plot of $C_t/C_0$ of MB versus reaction time showed that MB degrades from 54.8% (no catalyst) to 89.2%, 93.8%, and 78.4% for compound **1-3**, respectively, after 60 min irradiation (Fig. 6). In our previous research work, the [Cu*L*$_o$] species have been proved no catalytic activity in the dye degradation process.[26] Therefore, the Keggin-type Ti-substituted polyoxotungstate units in compounds **1-2** demonstrate better catalytic activities than those of typical Keggin-type polyoxotungstates in compound **3**. The stability of these hybrid compounds have been confirmed by the PXRD patterns (Fig. 7 and Fig. S17, ESI). After four cycles of photocatalytic degradation of MB, compounds **1-3** keep the similar catalytic activities and the structures have no change (Fig. S18-20).

Moreover, a supposed mechanism was proposed, involving that the UV-induced excited state POMs react with $H_2O$ to generate the active hydroxyl radical ($OH^{\bullet}$), which may oxidize the MB into the degradative products. Simultaneously, the reduced POM species were easily recovered into oxidative POMs by $O_2$ in the reaction system. The existence of active $OH^{\bullet}$ radicals in the reaction system was confirmed by the active species trapping experiments (as shown in Fig. S21). The photocatalytic MB degradation activities of compounds **1-2** (Ti-based POMs) were also compared with the P25-type titanium oxide. Both Ti-based POM compounds exhibit better catalytic activity than the one of P25(as shown in Fig. S22). Based on above experimental results, it can be presumed that the introduction of Ti elements into the POM structures may promote the electron transition and the easy generation of $OH^{\bullet}$ radicals. Moreover, the introduced Ti element may help the separation of photoelectron ($e^-$) and photohole ($h^+$), or the $Ti_2O$ group that introduced owns the photocatalytic activity, which can accelerate the photocatalyic MB degradation.

## Conclusions

In summary, we presented two new organic-inorganic hybrid compounds based on Ti-substituted POM units. In these compounds, the corner-sharing double-Keggin-type POM cluster is observed for the first time in the Ti-substituted POM species. The degradation of methylene blue (MB) under UV irradiation with compounds **1-3** proved that the Keggin-type Ti-substituted polyoxotungstates showed better photocatalytic activities than those of typical Keggin-type polyoxotungstate species. The introduction of potentially efficient POM species into the organic-inorganic hybrid compound systems may pave the ways for exploring new catalyst systems in UV-irradiated dye degradation. This work is ongoing in our group.

## Acknowledgements

This work was supported by National Natural Science Foundation of China (grant nos. 21271039, 21201032 and 21471028), Program for New Century Excellent Talents in University (grant no. NCET120813) and Fundamental Research Funds for the Central Universities (grant no. 11SSXT140).

## Notes and references

*Key Laboratory of Polyoxometalate Science of Ministry of Education, Department of Chemistry, Northeast Normal University, Changchun, 130024, P. R. China*
*E-mail: liyg658@nenu.edu.cn (Y.-G. Li) and zanghy100@nenu.edu.cn (H.-Y. Zang)*

† Electronic Supplementary Information (ESI) available: Summary of extra structural figures; selected bond lengths and angles; IR, TG and PXRD; photocatalytic experiments and cif files of **1**-**3**. CCDC reference numbers: 1039417 (**1**), 1039418 (**2**), and 1039419 (**3**). See DOI: 10.1039/b000000x/


1 L. Cronin and A. Müller, *Chem. Soc. Rev.*, 2012, **41**, 7333.
2 A. Dolbecq, E. Dumas, C. R. Mayer and P. Mialane, *Chem. Rev.*, 2010, **110**, 6009.
3 R. Yu, X. F. Kuang, X. Y. Wu, C. Z. Lu and J. P. Donahue, *Coord. Chem. Rev.*, 2009, **253**, 2872.
4 D. Y. Du, J. S. Qin, S. L. Li, Z. M. Su and Y. Q. Lan, *Chem. Soc. Rev.*, 2014, **43**, 4615.
5 X. J. Feng, Y. G. Li, Z. M. Zhang and E. B. Wang, *Acta. Chim. Sinica.*, 2013, **71**, 1575.
6 C. Zou, Z. J. Zhang, X. Xu, Q. H. Gong, J. Li and C. D. Wu, *J. Am. Chem. Soc.*, 2012, **134**, 87.
7 Z. Y. Fu, Y. Zeng, X. L. Liu, D. S. Song, S. J. Liao and J. C. Dai, *Chem. Commun.*, 2012, **48**, 6154.
8 X. L. Wang, X. J. Liu, A. X. Tian, J. Ying, H. Y. Lin, G. C. Liu and Q. Gao, *Dalton. Trans.*, 2012, **41**, 9587.
9 (a) X. L. Wang, D. Zhao, A. X. Tian and J. Ying, *Cryst. Eng. Comm.*, 2013, **15**, 4516; (b) X. L. Hao, Y. Y. Ma, W. Z. Zhou, H. Y. Zang, Y. H. Wang and Y. G. Li, *Chem. Asian. J.*, 2014, **9**, 3633; (c) X. L. Hao, Y. Y. Ma, Y. H. Wang, L. Y. Xu, F. C. Liu, M. M. Zhang and Y. G. Li, *Chem. Asian. J.*, 2014, **9**, 819.
10 X. Meng, C. Qin, X. L. Wang, Z. M. Su, B. Li and Q. H. Yang, *Dalton. Trans.*, 2011, **40**, 9964.
11 Y. Ding, J. X. Meng, W. L. Chen and E. B. Wang, *Cryst. Eng. Comm.*, 2011, **13**, 2687.
12 J. Lü, J. X. Lin, X. L. Zhao and R. Cao, *Chem. Comm.*, 2012, **48**, 669.
13 J. W. Zhao, D. Y. Shi, L. J. Chen, X. M. Cai, Z. Q. Wang, P. T. Ma, J. P. Wang and J. Y. Niu, *Cryst. Eng. Comm.*, 2012, **14**, 2797.
14 Q. Wu, W. L. Chen, D. Liu, C. Liang, Y. G. Li, S. W. Lin and E. B. Wang, *Dalton. Trans.*, 2011, **40**, 56.
15 (a) Y. Q. Chen, G. R. Li, Y. K. Qu, Y. H. Zhang, K. H. He, Q. Gao and X. H. Bu, *Cryst. Growth. Des.*, 2013, **13**, 901; (b) H. Y. Liu, L. Bo, J. Yang, Y. Y. Liu, J. F. Ma and H. Wu, Dalton. Trans., 2011, 40, 9782.
16 X. D. Yu, Y. N. Guo, L. L. Xu, X. Yang and Y. H. Guo, Colloids and Surfaces A: Physicochem. Eng. Aspects, 2008, 316, 110.
17 W. Guan, L. K. Yan, Z. M. Su, S. X. Liu, M. Zhang and X. H. Wang, Inorg. Chem., 2005, 44, 100.
18 K. Hayashi, M. Takahashi and K. Nomiya, Dalton.Trans., 2005, 23, 3751.
19 K. Hayashi, C. N. Kato, A. Shinohara, Y. Sakai and K. Nomiya, Journal of Molecular Catalysis A: Chemical, 2007, 262, 30
20 G. A. Al-Kadamany, F. Hussain, S. S. Mal, M. H. Dickman, N. Leclerc-Laronze, J. Marrot, E. Cadot and U. Kortz, Inorg. Chem., 2008, 47, 8574.
21 S. Yoshida, H. Murakami, Y. Sakai and K. Nomiya, Dalton. Trans., 2008, 34, 4630.
22 Y. Sakai, S. Ohta, Y. Shintoyo, S. Yoshida, Y. Taguchi, Y. Matsuki, S. Matsunaga and K. Nomiya, Inorg. Chem., 2011, 50, 6575.
23 Y. Sakai, K. Yoza, C. N. Kato and K. Nomiya, Chem. Eur. J., 2003, 9, 4077.
24 U. Kortz, S. S. Hamzeh and N. A. Nasser, Chem. Eur. J., 2003, 9, 2945.
25 Y. Sakai, K. Yoza, C. N. Kato and K. Nomiya, Dalton. Trans., 2003, 18, 3581.
26 X. Wang, M. M. Zhang, X. L. Hao, Y. H. Wang, Y. Wei, F. S. Liang, L. J. Xu and L. Y. Guang, Cryst. Growth. Des., 2013, 13, 3454.
27 P. J. Domaille and W. H. Knoth, Inorg. Chem., 1983, 22, 818.
28 J. S. Fleming, K. L. V. Mann, C. A. Carraz, E. Psillakis, J. C. Jeffery, J. A. McCleverty and M. D. Ward, Angew. Chem. Int. Ed., 1998, 37, 1279.
29 (a)G. M. Sheldrick, SHELXS-97, Program for solution of crystal structures, University of Göttingen, Germany, 1997; (b)G.M. Sheldrick, SHELXL-97, Program for refinement of crystal structures, University of Göttingen, Germany, 1997.
30 A.L. Spek, Acta Cryst., 2015, C71, 9.
31 (a)C. C. Chen, W. Zhao, P. X. Lei, J. C. Zhao and N. Serpone, Chem. Eur. J., 2004, 10, 1956; (b)H. B. Fu, C. S. Pan, W. Q. Yao and Y. F. Zhu, J. Phys. Chem. B., 2005, 109, 22432.

# Table of Contents

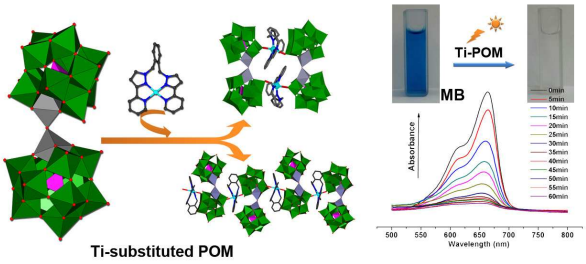


New organic-inorganic hybrid compounds based on Ti-substituted polyoxometalates exhibit high photocatalytic dye (MB) degradation activities.